JOURNAL OF THEORETICAL AND APPLIED MECHANICS
61, 3, pp. 419-426, Warsaw 2023
https://doi.org/10.15632/jtam-pl/165938

AN INVESTIGATION OF SPHERICAL MICRO/NANOPARTICLE MELTING USING ASYMPTOTIC MATCHINGS IN A WEAK FORMULATION

Yue Chan

Institute for Advanced Study, Shenzhen University, Nanshan District Shenzhen, Guangdong, China
e-mail: unimelbat@hotmail.com

In this paper, we investigate the speed of moving boundaries for melting micro/nanoparticles in the initial and final stages using asymptotic matchings in a weak formulation of the problem. We find that such a speed is initially proportional to the flux across the moving boundary, however a blowup occurs in a finite time when the surface tension is considered, both numerically and theoretically, by assuming linear relations between thermal conductivities and diffusivities, which paves the way to tackle the related two and higher phase change problems. Last but not least, we verify our theoretical outcomes using a quasi-stationary approximation approach.

Keywords: micro/nanoparticle, Stefan problem, blowup, weak formulation, asymptotic analysis

1. Introduction

Phase changes are ubiquitous in nature and technologies. Usually, bulk melting temperature is independent on its size. However, micro/nanoparticle melting temperature depends on its size owing to the higher value of surface by the volume ratio. Such an effect will lower the melting temperature (Buffat and Borel, 1976), which can be described by the Gibbs-Thomson equation (Langer, 1980) (see Eq. (2.3)). The lowering of the melting temperature will promote the molten speed, especially towards the final stage of the melting process resulting in blowing up the melting speed in a finite time (Herrero and Velázquez, 1996; McCue *et al.*, 2009) (see Fig. 2).

It is found that the prescribed Gibbs-Thomson condition at the solid-molten interface leads to mathematical complexity of solving the Stefan problems analytically (Carslaw and Jaeger, 1959; Crank, 1984) so that asymptotic techniques, for example using the large Stefan number (Davis and Hill, 1982; Herrero and Velázquez, 1997; Kucera and Hill, 1986; McCue *et al.*, 2008, 2009) and numerical methods (Crank, 1984; Meyer, 1973; Voller and Cross, 1981), are sought. The existence and uniqueness of certain functions related to phase-change problems are also studied (Ceretani *et al.*, 2020). Moreover, the Gibbs-Thomson condition imposed on the moving boundary poses difficulty on using the Baiocchi transform so that one can not employ the enthalpy method (Meyer, 1973; Voller and Cross, 1981) to tackle the governing equations numerically (McCue *et al.*, 2009). Due to the abundant aforementioned theoretical and numerical methods on solving the two-phase Stefan problems taking into account the surface tension, here, we extend our investigation by observing that such a condition can be naturally absorbed in the weak formulation (Evans, 2010; Roubiček, 2013) of the problem. Therefore, upon using asymptotic matchings, the retreating speed of the moving boundary at the initial and final stages can be estimated without directly solving the governing equations. We find that the initial speed depends linearly on the incoming heat flux at the boundary while the final speed will experience a finite time blowup, which is consistent with the existing literature (Herrero and Velázquez, 1996; McCue *et al.*, 2009).

In order to verify our outcomes, for simplicity, we assume that the solid temperature is constant. As the system is tiny, the molten temperature can reach quasi-stationary states after Δt so that a more complicated diffusion equation can be approximated by solving the Laplace equation at a certain time t (Howison, 2005; Yi, 2005). The molten temperature can then be solved using Eq. (3.1), from which the frontier of the moving boundary can be predicted iteratively by taking into account both the curvature and the surface tension, i.e. Eq. (3.2) by minimizing Eq. (3.3). The present author has successfully employed such methodology to scrutinize the effects of curvature and surface tension on the solidification of micro/nanoparticles, and designs certain smart materials (Gao *et al.*, 2023).

The structure of the present paper is organized as follows: governing equations for the present problem are given in Section 2, followed by a quasi-stationary approximation solution in Section 3. While weak formulations and a brief discussion of the existence of weak solutions are shown in Section 4, asymptotic analysis based on the weak formulations is ultimately made in the final Section.

2. Governing equations

Governing equations for both the molten and solid regimes by assuming axisymmetric micro/nano particles, are given below

$$\begin{aligned} \frac{\partial T_\ell(r,t)}{\partial t} &= \kappa_\ell\Big[\frac{\partial^2 T_\ell(r,t)}{\partial r^2} + \frac{2}{r}\frac{\partial T_\ell(r,t)}{\partial r}\Big] && R < r < a \\ \frac{\partial T_s(r,t)}{\partial t} &= \kappa_s\Big[\frac{\partial^2 T_s(r,t)}{\partial r^2} + \frac{2}{r}\frac{\partial T_s(r,t)}{\partial r}\Big] && 0 < r < R \end{aligned} \tag{2.1}$$

where $T_\ell(r,t)$, $T_s(r,t)$, κ_ℓ, κ_s denote the molten temperature, solid temperature, molten thermal diffusivity and solid thermal diffusivity, respectively. For simplicity, we drop (r,t) for $T_\ell(r,t)$ and $T_s(r,t)$. We comment that we investigate the simplest possible model in which no convective and source effects are imposed on the system. The schematic of the present problem is shown in Fig. 1.

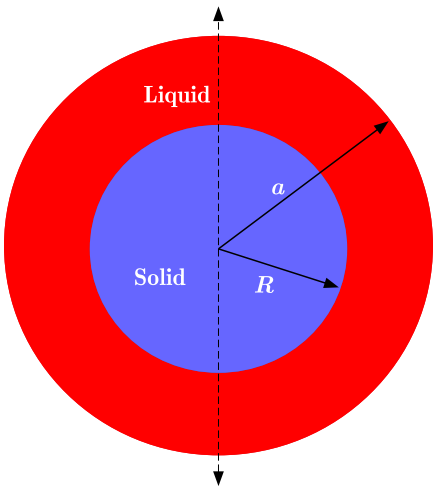

Fig. 1. Schematic diagram of the present melting process where the micro/nano particle is axisymmetric about the double arrow line

To obtain unique solutions of T_ℓ and T_s, both initial and boundary conditions including the Gibbs-Thomson moving boundary condition (Langer, 1980) are applied to give

$$\begin{aligned}
&\text{IC} \quad T_s = T_\ell \quad \text{on} \quad R(t=0) = a \\
&\text{BC} \quad T_\ell = T_a \quad \text{on} \quad r = a \qquad \frac{\partial T_s}{\partial r} = 0 \quad \text{on} \quad r = 0 \\
&\qquad T_\ell = T_s = T_f(R) \quad \text{on} \quad r = R(t) \\
&\text{MBC} \quad k_\ell \frac{\partial T_\ell}{\partial r} - k_s \frac{\partial T_s}{\partial r} = -\rho_\ell \frac{dR(t)}{dt}[(c_\ell - c_s)(T_f(R) - T_m) + L] \quad \text{on} \quad r = R(t)
\end{aligned} \tag{2.2}$$

where k_ℓ, k_s, ρ_ℓ, c_ℓ, c_s, T_f, T_m and L denote the thermal conductivity of the liquid, thermal conductivity of the solid, density of the material, specific heat capacity of the liquid, specific heat capacity of the solid, curvature dependent temperature of the melting point, melting temperature and latent heat, respectively. For simplicity, we drop (t) for $R(t)$. We also note that $T_s \leqslant T_\ell \leqslant T_a$.

In addition, the curvature-dependent melting point, known as the Gibbs-Thomson effect, which basically implies a modification (decrease) of the melting temperature by surface tension, is defined below

$$T_f(R) = T_m\Big(1 - \frac{\omega}{R}\Big) \qquad \omega = \frac{2\sigma}{\rho_s L} \tag{2.3}$$

where σ and ρ_s further denote the interfacial tension coefficient and mass density of the solid, respectively. In addition, capillary pressure is radially dependent due to the term ω/R.

3. Quasi-stationary approximation simulation

To simulate the melting process, instead of solving more complicated diffusion equations, i.e. Eq. (2.1), we adopt a quasi-approximation approach, where we assume that the system and the Peclet number are tiny that it can reach a quasi-stationary state (Howison, 2005) for each time step so that the time evolution of the moving boundary can be updated by simulations (3.4). We assume T_s is constant for all times, which is valid due to the tiny size of particles as well as the satisfaction of Eq. (2.1) as well as the boundary conditions. The aforementioned assumptions will be relaxed in the later Sections. Using separation of variables, we obtain a general solution of T_ℓ, which is given by

$$T_\ell = \mathrm{e}^{\lambda t}\left[\frac{A\sinh\Big(\sqrt{\frac{\lambda}{\kappa_\ell}}r\Big) + B\cosh\Big(\sqrt{\frac{\lambda}{\kappa_\ell}}r\Big)}{r}\right] \tag{3.1}$$

where λ is the separation constant yet to be determined by the boundary conditions. Moreover, λ, A and B are to be obtained from the initial and boundary conditions excluding the moving boundary, which are given below

$$\begin{aligned}
&\frac{A\sinh\Big(\sqrt{\frac{\lambda}{\kappa_\ell}}a\Big) + B\cosh\Big(\sqrt{\frac{\lambda}{\kappa_\ell}}a\Big)}{a} = T_s \\
&\mathrm{e}^{\lambda t}\left[\frac{A\sinh\Big(\sqrt{\frac{\lambda}{\kappa_\ell}}a\Big) + B\cosh\Big(\sqrt{\frac{\lambda}{\kappa_\ell}}a\Big)}{a}\right] = T_a \\
&\mathrm{e}^{\lambda t}\left[\frac{A\sinh\Big(\sqrt{\frac{\lambda}{\kappa_\ell}}R\Big) + B\cosh\Big(\sqrt{\frac{\lambda}{\kappa_\ell}}R\Big)}{R}\right] = T_f(R)
\end{aligned} \tag{3.2}$$

To maintain the compatibility of the first and second equations of Eq. (3.2), we can estimate λ as $\lambda = (1/a)\log(T_a/T_s)$, which makes sense when a temporal change in the molten temperature depends on temperature differences between the embedding environment and solid temperature.

It also depends on how big a micro/nanoparticle is. Therefore, the conditions of Eq. (3.2) reduce from three to two. R is still unresolved, however the moving boundary condition provides an extra condition to save us

$$\min_{0\leqslant R\leqslant a}\left\{\left|k_\ell\frac{\partial T_\ell}{\partial r}+\rho_\ell\frac{a-R}{\Delta t}[(c_\ell-c_s)(T_f(R)-T_m)+L]\right|\right\} \tag{3.3}$$

Now, Eqs. (3.2) and (3.3) can be used to obtain A, B and R. Since multiple solutions are possible, we only select A and B, when R is close to a when a tiny time is chosen. Given that the trace of the moving boundary can be estimated using the modified Euler method taking both the speed and curvature into account

$$R_{n+1}=R_n+\Delta t\frac{dR_n}{dt}+\frac{\Delta t^2}{2!}\frac{d^2R_n}{dt^2} \tag{3.4}$$

where n denotes the number of iterations to trace the moving boundary. We firstly use Eq. (3.4) to simulate the moving boundary of gold microparticles of the size 1 nm using the parameters given in Table 1. In addition, we let $T_s=300\,\mathrm{K}$ and $T_a=2000\,\mathrm{K}$. Using Eqs. (3.2) and (3.3), the coefficients A and B for gold are estimated to be -0.58822 and 0.00124, respectively. From which, we can first estimate $\lambda=0.1897\cdot10^7$. Parameters for Sn and Pb can be found in Table 1. Now, we adopt Eq. (3.4) to simulate the location of the moving boundaries for the proposed metals, where the numerical results are shown in Fig. 2.

Table 1. Parameters for Au, Sn and Pb (McCue *et al.*, 2009)

Parameters	Gold	Sn	Pb
ρ_s	$19.3\cdot10^3\,\mathrm{kg/m^3}$	$7.27\cdot10^3\,\mathrm{kg/m^3}$	$11.34\cdot10^3\,\mathrm{kg/m^3}$
ρ_ℓ	$17.31\cdot10^3\,\mathrm{kg/m^3}$	$6.99\cdot10^3\,\mathrm{kg/m^3}$	$10.66\cdot10^3\,\mathrm{kg/m^3}$
L	63718 J/kg	59225 J/kg	23020 J/kg
T_m	1337.3 K	505.8 K	600.6 K
ω	0.2396 nm	0.4447 nm	0.6847 nm
$\kappa_\ell=k_\ell/(\rho_\ell c_\ell)$	$1.47\cdot10^{-3}\,\mathrm{m^2/s}$	$1.36\cdot10^{-3}\,\mathrm{m^2/s}$	$0.684\cdot10^{-3}\,\mathrm{m^2/s}$
k_ℓ	320 W/(m·K)	67 W/(m·K)	35 W/(m·K)
c_s	0.128 J/gK	0.226 J/gK	0.13 J/gK
c_ℓ	12.55 J/gK	7.029 J/gK	4.799 J/gK

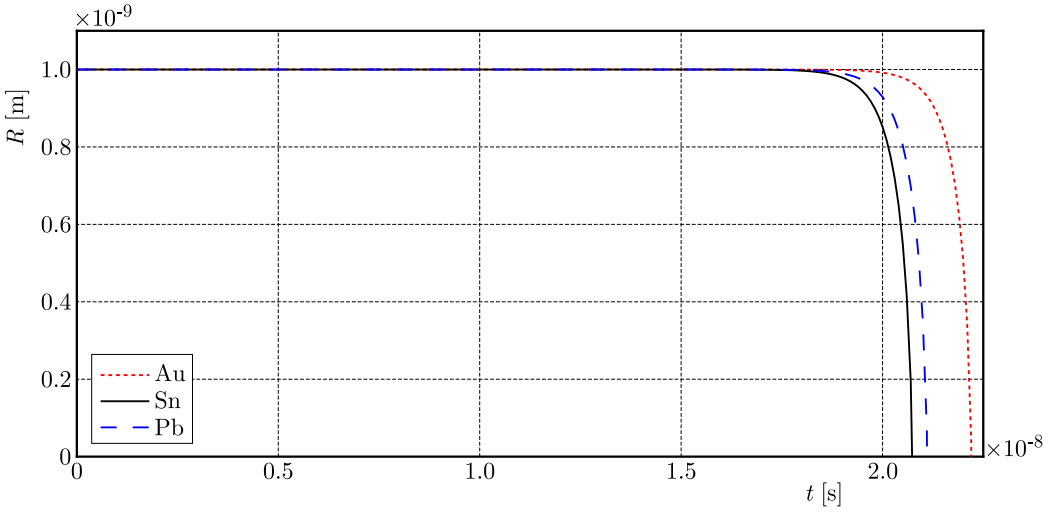

Fig. 2. Melting process for Au, Sn and Pb

We can observe from Fig. 2 that the moving boundaries retreat steadily or initially linearly but accelerate rapidly, even with a blowup after $2\cdot 10^{-8}$ s. Such behavior will be fully scrutinized in Section 5.

4. Weak formulation

A weak formulation forms a basis for seeking weak solutions and the finite element method. In this Section, we determine the weak formulation of Eq. (2.1). Upon multiplying both sides of Eq. (2.1) by $v \in C^{\infty}(I, V)$, where I and V denote the usual temporal and spatial domains, respectively, and upon integrating by parts and applying appropriate boundary conditions at R and a, we obtain

$$\int_R^a \frac{\partial T_\ell}{\partial t} v \, dr = -\kappa_\ell \left(v \frac{\partial T_\ell}{\partial r}\Big|_R + \int_R^a \frac{\partial T_\ell}{\partial r}\frac{\partial v}{\partial r} \, dr - 2\int_R^a \frac{v}{r}\frac{\partial T_\ell}{\partial r} d\, r \right) \tag{4.1}$$

Similarly, we obtain the weak formulation for T_s

$$\int_0^R \frac{\partial T_s}{\partial t} v \, dr = \kappa_s \left(v \frac{\partial T_s}{\partial r}\Big|_R - \int_0^R \frac{\partial T_s}{\partial r}\frac{\partial v}{\partial r} \, dr + 2\int_0^R \frac{v}{r}\frac{\partial T_s}{\partial r} \, dr \right) \tag{4.2}$$

where the weak solutions for Eqs. (4.1) and (4.2) have been thoroughly studied using the coercivity of T_ℓ and T_s, the first temporal derivatives, proper growth conditions and pseudomonotonic or weakly continuous approaches for the nonlinearity (Roubiček, 2013).

5. Asymptotic analysis

Now we relax that T_s is a constant and illustrate the asymptotic behavior of the moving boundary using an energy method as given in the previous Section. Replacing v in Eqs. (4.1) and (4.2) by T_ℓ and T_s, respectively, we obtain

$$\begin{aligned} \frac{1}{2}\frac{\partial}{\partial t}\|T_\ell\|^2_{L^2(R)} &= -\kappa_\ell \left(T_f(R)\frac{\partial T_\ell}{\partial r}\Big|_R + \|T_\ell\|^2_{H^1(R)} - 2\int_R^a \frac{T_\ell}{r}\frac{\partial T_\ell}{\partial r} \, dr \right) \\ \frac{1}{2}\frac{\partial}{\partial t}\|T_s\|^2_{L^2(R)} &= \kappa_s \left(T_f(R)\frac{\partial T_s}{\partial r}\Big|_R - \|T_s\|^2_{H^1(R)} + 2\int_0^R \frac{T_s}{r}\frac{\partial T_s}{\partial r} \, dr \right) \end{aligned} \tag{5.1}$$

where we have used the boundary conditions that $T_\ell = T_s = T_f(R)$ on $r = R(t)$ to obtain Eq. (5.1). For simplicity, we have dropped the notation of temporal and spatial domains. The values in $H(\cdot)$ denote the integration limit for integrals in Eqs. (4.1) and (4.2), where $R \in [0, a]$.

— In the **initial stage**, since the molten state is completely absent, we have

$$\frac{1}{2}\frac{\partial}{\partial t}\|T_s\|^2_{L^2(a)} = \kappa_s \left(T_f(a)\frac{\partial T_s}{\partial r}\Big|_a - \|T_s\|^2_{H^1(a)} + 2\int_0^a \frac{T_s}{r}\frac{\partial T_s}{\partial r} \, dr \right) \tag{5.2}$$

— In the **final stage**, since the condensed state is completely absent, we have

$$\frac{1}{2}\frac{\partial}{\partial t}\|T_\ell\|^2_{L^2(0)} = -\kappa_\ell \left(T_f(0)\frac{\partial T_\ell}{\partial r}\Big|_0 + \|T_\ell\|^2_{H^1(0)} - 2\int_0^a \frac{T_\ell}{r}\frac{\partial T_\ell}{\partial r} \, dr \right) \tag{5.3}$$

— In the **intermediate stage**, both the solid and molten stages coexist so that by using Eq. (5.1) the change in total kinetic energies for both the solid and molten regimes is obtained

$$\begin{aligned}
&\frac{1}{2}\frac{\partial}{\partial t}\Big(\|T_\ell\|^2_{L^2(R)}+\|T_s\|^2_{L^2(R)}\Big)=-T_f(R)\bigg[\kappa_\ell\frac{\partial T_\ell}{\partial r}\Big|_R-\kappa_s\frac{\partial T_s}{\partial r}\Big|_R\bigg]\\
&\quad-\kappa_\ell\|T_\ell\|^2_{H^1(R)}-\kappa_s\|T_s\|^2_{H^1(R)}+2\bigg(\kappa_s\int_0^R\frac{T_s}{r}\frac{\partial T_s}{\partial r}\,dr+\kappa_\ell\int_R^a\frac{T_\ell}{r}\frac{\partial T_\ell}{\partial r}\,dr\bigg)\\
&\quad\approx-T_f(R)\rho_\ell\frac{dR}{dt}\Big[(c_\ell-c_s)\Big(\frac{T_m\omega}{R}\Big)-L\Big]-\kappa_\ell\|T_\ell\|^2_{H^1(R)}-\kappa_s\|T_s\|^2_{H^1(R)}\\
&\quad+2\bigg(\kappa_s\int_0^R\frac{T_s}{r}\frac{\partial T_s}{\partial r}\,dr+\kappa_\ell\int_R^a\frac{T_\ell}{r}\frac{\partial T_\ell}{\partial r}\,dr\bigg)
\end{aligned}\tag{5.4}$$

where we have assumed $\kappa_\ell\approx k_\ell$ and $\kappa_s\approx k_s$ (or else if there are linear relations between thermal diffusivities and conductivities). We comment that there is a common relation between them for simple metals, i.e. $\kappa_i=k_i/(\rho_i c_i)$, where $i=s,\ell$ (McCue *et al.*, 2009), and the moving boundary condition is imposed in the second equation of Eq. (5.4). We might make rather restrictive assumptions here for mathematical convenience as we can yield dR/dt and make certain simplifications using the moving boundary condition as given in Eq. (2.2). Now, the asymptotic speed of the moving boundary condition can be matched with the melting speeds of the initial and final stages.

— In the **nearly initial stage**, upon ignoring T_ℓ, Eq. (5.4) becomes

$$\begin{aligned}
&\frac{1}{2}\frac{\partial}{\partial t}\|T_s\|^2_{L^2(a)}=-T_f(a)\rho_\ell\frac{dR}{dt}\Big[(c_\ell-c_s)\Big(\frac{T_m\omega}{a-\varepsilon}\Big)-L\Big]-\kappa_s\|T_s\|^2_{H^1(a)}+2\kappa_s\int_0^{a-\varepsilon}\frac{T_s}{r}\frac{\partial T_s}{\partial r}\,dr\\
&\quad\approx-T_f(a)\rho_\ell\frac{dR}{dt}\Big[\frac{(c_\ell-c_s)T_m\omega}{a}\Big(1+\frac{\varepsilon}{a}\Big)-L\Big]-\kappa_s\|T_s\|^2_{H^1(a)}\\
&\quad+2\kappa_s\int_0^a\frac{T_s}{r}\frac{\partial T_s}{\partial r}\,dr+O(\varepsilon^2)
\end{aligned}\tag{5.5}$$

where ε denotes an infinitesimal positive number. Now comparing Eq. (5.5) with Eq. (5.2), we obtain

$$\frac{dR}{dt}=-\frac{\kappa_s a}{\rho_\ell}\Big[\frac{1}{(c_\ell-c_s)T_m\omega-aL}\Big]\frac{\partial T_s}{\partial r}\Big|_a+O(\varepsilon)\tag{5.6}$$

Hence, the melting speed is linearly proportional to the heat flux across the boundary. We comment that in this formulation, whether the initial temperature is fusion or not, (Kucera and Hill, 1986) it is not crucial.

— In the **nearly melting stage**, upon ignoring T_s and matching Eq. (5.4) with Eq. (5.3), we obtain

$$\frac{dR}{dt}=\frac{\kappa_\ell}{\rho_\ell}\Big[(c_\ell-c_s)\frac{T_m\omega}{\varepsilon}-L\Big]^{-1}\frac{\partial T_\ell}{\partial r}|_\varepsilon\tag{5.7}$$

where the melting speed blows up when

$$\varepsilon^*=\frac{(c_\ell-c_s)T_m\omega}{L}\tag{5.8}$$

Hence, we can observe from Eq. (5.8) that no blowup is observed when the surface tension is zero happening in the macroscopic melting problems. Figure 2 confirms the linear correlation with the temperature flux and the blowup in the initial and final stages, respectively. ε^* is $0.62466 \cdot 10^{-10}$ m, $0.25837 \cdot 10^{-10}$ m and $0.83407 \cdot 10^{-10}$ m for Au, Sn and Pb, respectively, which partially agrees with Fig. 2, where Sn supposes to melt the slowest but it melts the fastest simply due to the fact that we neglect the heat transfer in the sold regime when we conduct the quasi-stationary approach.

6. Conclusion

Using the weak formulation of the Stefan problem and asymptotic matchings, we find that the retreating speed of the moving boundary of spherical micro/nanoparticles depends initially linearly on the incoming heat flux but blows up in the finite time at the latter stage without solving the original equations. No boundary problem occurs as the boundary conditions are absorbed naturally in the weak formulation. Such techniques can be employed to two and multi-phase change problems. A quasi-stationary approximation has also been employed to verify the claims of our theoretical results.

Acknowledgements

This research was financially supported by Shenzhen Basic Research Program under Grant No. JCYJ20190808144813101, Shenzhen High-end Talent Scheme under Grant No. 827/000567, Shenzhen University Starting Up Fund Grant No. 860/000002110377 and Shenzhen University Key Project Grant No. 860-000002081303.

References

1. Buffat P.A., Borel J.P., 1976, Size effect on the melting temperature of gold particles, *Physical Review A*, **13**, 2287-2298
2. Carslaw H.S., Jaeger J.C., 1959, *Conduction of Heat in Solids*, Clarendon, Oxford
3. Ceretani A.N., Salva N.N., Tarzia D.A., 2020, Auxiliary functions in the study of Stefan-like problems with variable thermal properties, *Applied Mathematics Letters*, **104**, 106204
4. Crank J., 1984, *Free and Moving Boundary Problems*, Clarendon, Oxford
5. Davis G.B., Hill J.M., 1982, A moving boundary problem for the sphere, *IMA Journal of Applied Mathematics*, **29**, 99-111
6. Evans L.C., 2010, *Nonlinear Partial Differential Equations*, American Mathematical Society, Berkeley
7. Gao J., Chan Y., Hou T., Ren Y., 2023, Quasi-equilibrium approximation of the solidification process for micro phase change materials taking into account curvature and surface tension, *International Journal of Thermal Sciences*, **184**, 107916
8. Herrero M.A., Velázquez J.J.L., 1996, Singularity formation in the one-dimensional supercooled Stefan problem, *European Journal of Applied Mathematics*, **7**, 119-150
9. Herrero M.A., Velázquez J.J.L., 1997, On the melting of ice balls, *SIAM Journal on Mathematical Analysis*, **28**, 1-32
10. Howison S., 2005, *Practical Applied Mathematics*, Cambridge University Press
11. Kucera A., Hill J.M., 1986, On inward solidifying cylinders and spheres initially not at their fusion temperature, *International Journal of Non-Linear Mechanics*, **21**, 73-82

12. Langer J.S., 1980, Instabilities and pattern formation in crystal growth, *Reviews of Modern Physics*, **52**, 81-94

13. McCue S.W., Wu B., Hill J.M., 2008, Classical two-phase Stefan problem for spheres, *Proceedings of the Royal Society A*, **464**, 2055-2076

14. McCue S.W., Wu B., Hill J.M., 2009, Micro/nanoparticle melting with spherical symmetry and surface tension, *IMA Journal of Applied Mathematics*, **74**, 439-457

15. Meyer G.H., 1973, Multidimensional Stefan problems, *SIAM Journal on Numerical Analysis*, **10**, 522-538

16. Roubiček T., 2013, *Nonlinear Partial Differential Equations with Applications*, Birkhauser, Basel

17. Voller V., Cross M., 1981, Accurate solutions of moving boundary problems using the enthalpy method, *International Journal of Heat and Mass Transfer*, **24**, 545-556

18. Yi F., 2005, Global classical solution of quasi-stationary Stefan free boundary problem, *Applied Mathematics and Computation*, **160**, 797-817

Manuscript received February 15, 2023; accepted for print March 29, 2023